

Received 23 April 2024
Accepted 14 June 2024

Edited by J. Ellena, Universidade de São Paulo,
Brazil

Keywords: crystal structure; acylation;
thienylallylamines; maleic acid amide; weak
interactions; Hirshfeld surface analysis.

CCDC reference: 2362911

Supporting information: this article has
supporting information at journals.iucr.org/e

Crystal structure and Hirshfeld surface analysis of 1-[6-bromo-2-(4-fluorophenyl)-1,2,3,4-tetrahydroquinolin-4-yl]pyrrolidin-2-one

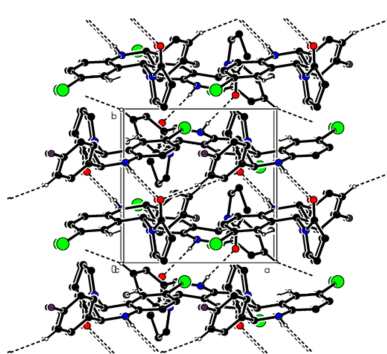
Anastasia A. Pronina,^a Alexandra G. Podrezova,^a Mikhail S. Grigoriev,^b Khudayar I. Hasanov,^{c,d} Nurlana D. Sadikhova,^e Mehmet Akkurt^{f*} and Ajaya Bhattacharai^{g*}

^aRUDN University, 6 Miklukho-Maklaya St., Moscow, 117198, Russian Federation, ^bFrumkin Institute of Physical Chemistry and Electrochemistry, Russian Academy of Sciences, Leninskiy prospect 31-4, Moscow 119071, Russian Federation, ^cWestern Caspian University, Iстиqlaliyat Street 31, AZ1001, Baku, Azerbaijan, ^dAzerbaijan Medical University, Scientific Research Centre (SRC), A. Kasumzade St. 14. AZ 1022, Baku, Azerbaijan, ^eDepartment of Chemistry, Baku State University, Z. Xalilov Str, Az 1148 Baku, Azerbaijan, ^fDepartment of Physics, Faculty of Sciences, Erciyes University, 38039 Kayseri, Türkiye, and ^gDepartment of Chemistry, M.M.A.M.C (Tribhuvan University) Biratnagar, Nepal. *Correspondence e-mail: akkurt@erciyes.edu.tr, ajaya.bhattacharai@mamc.tu.edu.np

In the title compound, $C_{19}H_{18}BrFN_2O$, the pyrrolidine ring adopts an envelope conformation. In the crystal, molecules are linked by intermolecular $N-H\cdots O$, $C-H\cdots O$, $C-H\cdots F$ and $C-H\cdots Br$ hydrogen bonds, forming a three-dimensional network. In addition, $C-H\cdots \pi$ interactions connect molecules into ribbons along the *b*-axis direction, consolidating the molecular packing. The intermolecular interactions in the crystal structure were quantified and analysed using Hirshfeld surface analysis.

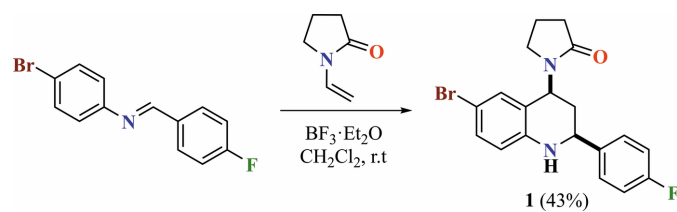
1. Chemical context

As a result of their presence in many plants, tetrahydroquinoline derivatives have long been of great interest to organic chemists and biochemists. The tetrahydroquinoline moiety can be found in many alkaloids that possess antimalarial and antimicrobial properties (Ghashghaei *et al.*, 2018; Khalilov *et al.*, 2021; Safavora *et al.*, 2019). Various studies show that tetrahydroquinolines have a wide spectrum of biological activity, and some are already being used as pharmaceutical agents (Sridharan *et al.*, 2011; Akbari Afkhami *et al.*, 2017; Abdelhamid *et al.*, 2011). Modification of tetrahydroquinoline derivatives is effective in the search, design, and development of new drugs. However, thousands of compounds are required to find a structure that exhibits biological activity, which is why an efficient synthetic methodology for obtaining tetrahydroquinoline derivatives is necessary (Astudillo *et al.*, 2009; Kouznetsov *et al.*, 2004, 2007). One of the most widely used approaches for the synthesis of tetrahydroquinolines is the Povarov reaction, known as the aza-Diels–Alder reaction (Palacios *et al.*, 2010; Zubkov *et al.*, 2010; Zaitsev *et al.*, 2009). Herein, we have synthesized 1-[6-bromo-2-(4-fluorophenyl)-1,2,3,4-tetrahydroquinolin-4-yl]pyrrolidin-2-one (**I**) by the reaction of (*E*)-*N*-(4-bromophenyl)-1-(4-fluorophenyl)methanimine with 1-vinylpyrrolidin-2-one in the presence of the most commonly used Lewis acid, diethyl ether of boron trifluoride (Fig. 1). The mild conditions and efficiency of the cycloaddition of aromatic imines with electronically enriched alkenes make the Povarov reaction a useful tool in the synthesis of tetrahydroquinolines, optimization of the search for potential drugs, and obtaining hits. It should be mentioned that the conformation of the obtained



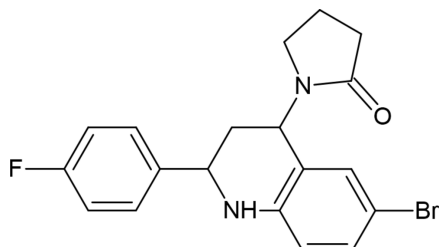
OPEN ACCESS

Published under a CC BY 4.0 licence

**Figure 1**

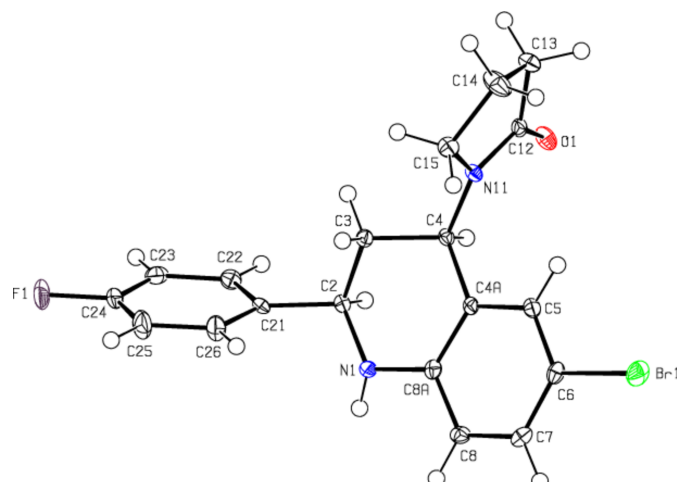
Synthesis of 1-[6-bromo-2-(4-fluorophenyl)-1,2,3,4-tetrahydroquinolin-4-yl]pyrrolidin-2-one (I).

1,2,3,4-tetrahydroquinoline cycle plays a key role in the biological activity of a potential drug. The attached halogens ($-F$ and $-Br$) as well as NH or $\text{C}=\text{O}$ groups can participate in various sorts of intermolecular interactions (Gurbanov *et al.*, 2020, 2022*a,b*; Kopylovich *et al.*, 2011*a,b*; Mahmoudi *et al.*, 2017*a,b*), which can improve the solubility of this compound. Thus, this communication is devoted to the elucidation of the spatial peculiarities of the partly hydrogenated quinoline fragment in the products of the Povarov reaction.



2. Structural commentary

In the title compound (Fig. 2), the 1,2,3,4-tetrahydropyridine ring ($\text{N}1/\text{C}2-\text{C}4/\text{C}4\text{A}/\text{C}8\text{A}$) of the 1,2,3,4-tetrahydroquinoline ring system ($\text{N}1/\text{C}2-\text{C}4/\text{C}4\text{A}/\text{C}5-\text{C}8/\text{C}8\text{A}$) adopts an envelope conformation [the puckering parameters (Cremer & Pople, 1975) are $Q_T = 0.509$ (2) \AA , $\theta = 46.3$ (2) $^\circ$, $\varphi = 121.4$ (3) $^\circ$], while

**Figure 2**

View of the title molecule. Displacement ellipsoids are drawn at the 50% probability level.

Table 1
Hydrogen-bond geometry (\AA , $^\circ$).

$Cg3$ is the centroid of the $\text{C}4\text{A}/\text{C}5-\text{C}8/\text{C}8\text{A}$ ring.

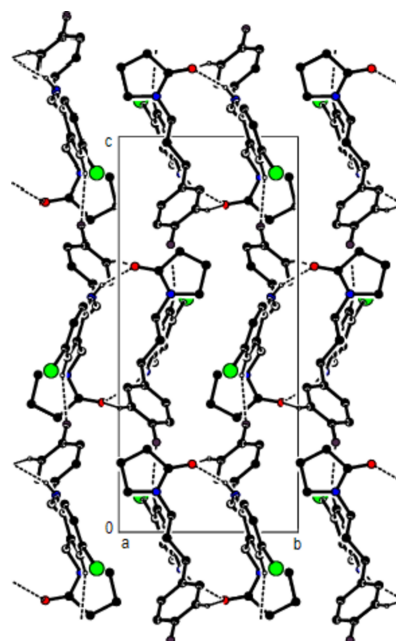
$D-\text{H}\cdots A$	$D-\text{H}$	$\text{H}\cdots A$	$D\cdots A$	$D-\text{H}\cdots A$
$\text{N}1-\text{H}1\cdots \text{O}1^i$	0.85 (2)	2.43 (2)	3.217 (2)	154 (2)
$\text{C}5-\text{H}5\text{A}\cdots \text{F}1^{ii}$	0.95	2.50	3.393 (2)	157
$\text{C}23-\text{H}23\text{A}\cdots \text{O}1^{iii}$	0.95	2.46	3.365 (2)	159
$\text{C}15-\text{H}15\text{B}\cdots \text{Br}1^{iv}$	0.99	2.98	3.703 (2)	131
$\text{C}2-\text{H}2\text{A}\cdots \text{Cg}3^i$	1.00	2.68	3.676 (2)	172
$\text{C}15-\text{H}15\text{A}\cdots \text{Cg}3^v$	0.99	2.94	3.386 (2)	109
$\text{C}15-\text{H}15\text{B}\cdots \text{Cg}3^v$	0.99	2.97	3.386 (2)	106

Symmetry codes: (i) $-x+1, -y, -z+1$; (ii) $x-\frac{1}{2}, -y+\frac{1}{2}, z+\frac{1}{2}$; (iii) $-x+2, -y, -z+1$; (iv) $x+1, y, z$; (v) $-x+1, -y+1, -z+1$.

the benzene ring ($\text{C}4\text{A}/\text{C}5-\text{C}8/\text{C}8\text{A}$) is essentially planar (r.m.s. deviation = 0.002 \AA). The plane (r.m.s. deviation = 0.002 \AA) of the 1,2,3,4-tetrahydroquinoline ring system forms angles of 65.91 (8) and 81.17 (9) $^\circ$, respectively, with the fluorobenzene ring ($\text{C}21-\text{C}26$) and the pyrrolidine ring ($\text{N}11/\text{C}12-\text{C}15$) (r.m.s. deviation = 0.002 \AA), which has an envelope conformation [the puckering parameters are $Q(2) = 0.195$ (2) \AA , $\varphi(2) = 107.4$ (6) $^\circ$]. The angle between the pyrrolidine and fluorobenzene rings is 71.16 (11) $^\circ$. The geometric parameters in the molecule are normal and in good agreement with those in the compounds discussed in the Database survey section.

3. Supramolecular features and Hirshfeld surface analysis

In the crystal, molecules are linked by intermolecular $\text{N}-\text{H}\cdots \text{O}$, $\text{C}-\text{H}\cdots \text{O}$, $\text{C}-\text{H}\cdots \text{F}$ and $\text{C}-\text{H}\cdots \text{Br}$ hydrogen bonds, forming a three-dimensional network (Table 1; Figs. 3,

**Figure 3**

A view of the molecular packing along the a axis of the title compound, showing the $\text{N}-\text{H}\cdots \text{O}$, $\text{C}-\text{H}\cdots \text{O}$, $\text{C}-\text{H}\cdots \text{F}$ and $\text{C}-\text{H}\cdots \text{Br}$ hydrogen bonds.

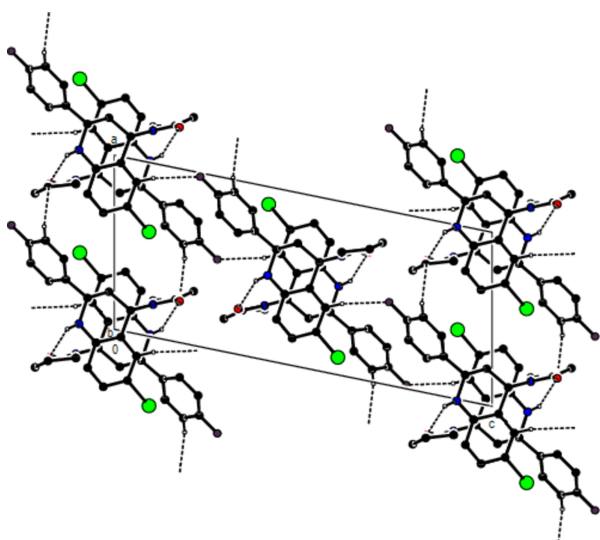


Figure 4
A view of the molecular packing along the *b* axis of the title compound.

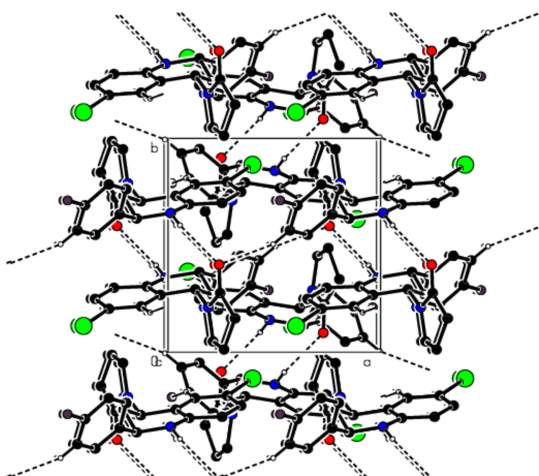


Figure 5
A view of the molecular packing along the *c* axis of the title compound.

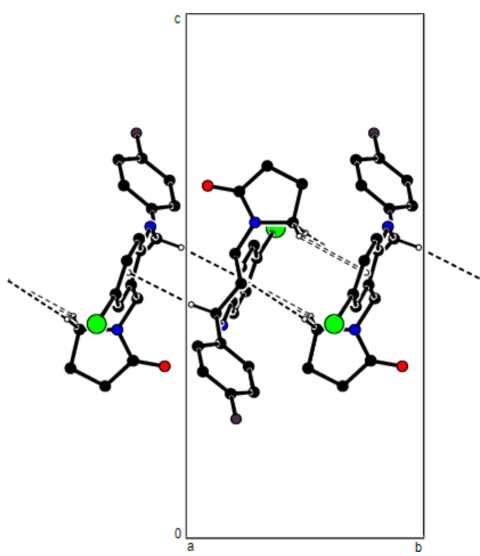


Figure 6
A view of the molecular packing along the *a* axis of the title compound, showing the C–H···π interactions.

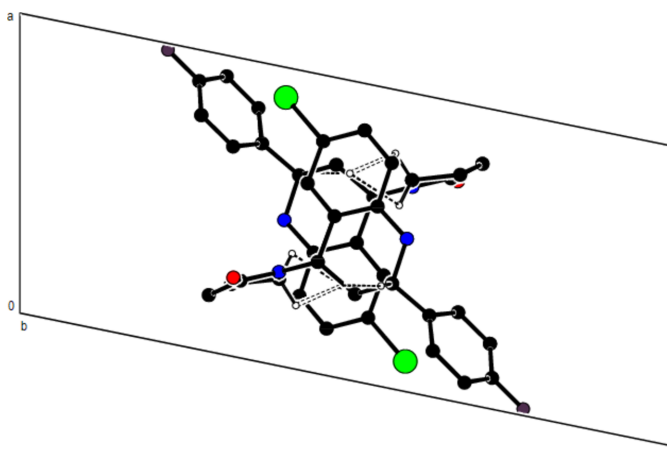


Figure 7
A view of the molecular packing along the *b* axis.

4 and 5). In addition, C–H···π interactions connect molecules, forming ribbons along the *b*-axis direction and consolidating molecular packing (Table 1; Figs. 6, 7 and 8).

To quantify the intermolecular interactions in the crystal, the Hirshfeld surfaces of the title molecule and the two-dimensional fingerprints were generated with *Crystal-Explorer17.5* (Spackman *et al.*, 2021). The d_{norm} mappings for the title compound were performed in the range -0.2398 (red) to $+1.3617$ (blue). On the d_{norm} surfaces, bright-red spots show the locations of the N–H···O, C–H···O and C–H···F interactions (Table 1; Fig. 9*a,b*).

The overall two-dimensional fingerprint plot for the title compound and those delineated into H···H (Fig. 10*b*; 38.7%),

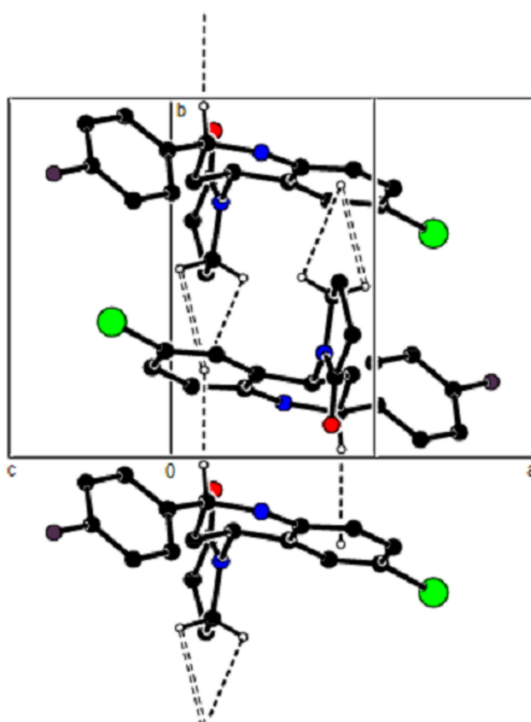
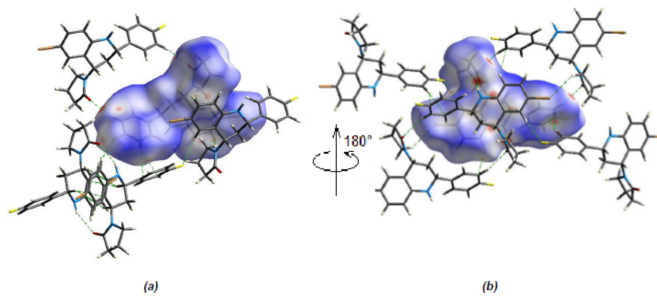


Figure 8
A view of the molecular packing of the title compound showing supramolecular ribbons running along the *c*-axis direction.

**Figure 9**

(a) Front and (b) back views of the three-dimensional Hirshfeld surface for the title compound. Some $\text{N}-\text{H}\cdots\text{O}$, $\text{C}-\text{H}\cdots\text{O}$ and $\text{C}-\text{H}\cdots\text{F}$ interactions are shown as dashed lines.

$\text{C}\cdots\text{H}/\text{H}\cdots\text{C}$ (Fig. 10c; 24.3%), $\text{Br}\cdots\text{H}/\text{H}\cdots\text{Br}$ (Fig. 10d; 14.9%) and $\text{F}\cdots\text{H}/\text{H}\cdots\text{F}$ (Fig. 10e; 9.6%) contacts are shown in Fig. 10. $\text{O}\cdots\text{H}/\text{H}\cdots\text{O}$ (8.8%), $\text{Br}\cdots\text{C/C}\cdots\text{Br}$ (1.8%),

$\text{F}\cdots\text{O}/\text{O}\cdots\text{F}$ (0.6%), $\text{F}\cdots\text{C/C}\cdots\text{F}$ (0.6%), $\text{N}\cdots\text{H}/\text{H}\cdots\text{N}$ (0.5%), $\text{Br}\cdots\text{N/N}\cdots\text{Br}$ (0.1%) and $\text{Br}\cdots\text{Br}$ (0.1%) contacts have little directional influence on the molecular packing.

4. Database survey

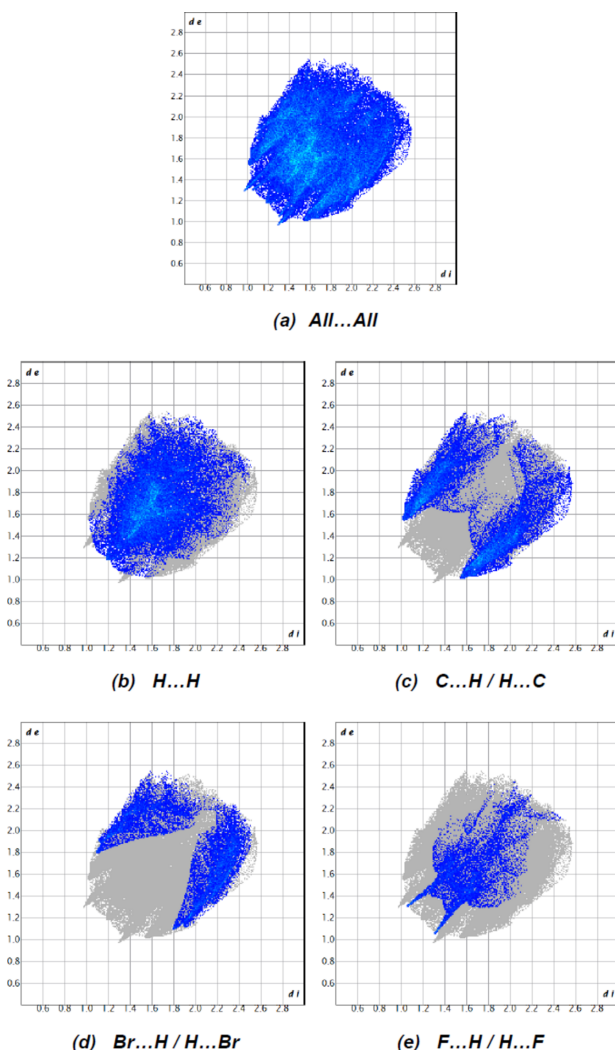
A search of the Cambridge Structural Database (CSD, Version 5.42, update of September 2021; Groom *et al.*, 2016) for similar structures with the 1,2,3,4-tetrahydroquinoline unit showed that the six most closely related species to the title compound are those with refcodes WACWOO (Çelik *et al.*, 2010a), CEDNUW (Çelik *et al.*, 2010b), SUFDEE (Jeyaseelan, *et al.*, 2015c), NOVGAI (Jeyaseelan *et al.*, 2015a), WUFBEG (Jeyaseelan *et al.*, 2015b) and EZOMIR (Çelik *et al.*, 2016).

The crystal structure of WACWOO is consolidated by weak aromatic $\pi-\pi$ interactions [centroid–centroid distance = 3.802 (4) Å] between the pyridine and benzene rings of the quinoline ring systems of adjacent molecules. In the crystal of CEDNUW, $\pi-\pi$ stacking interactions are present between the pyridine and benzene rings of adjacent molecules [centroid–centroid distances = 3.634 (4) Å], and short $\text{Br}\cdots\text{Br}$ contacts [3.4443 (13) Å] occur. In the crystal of SUFDEE, molecules are linked by weak $\text{C}-\text{H}\cdots\text{O}$ hydrogen bonds, generating $C(8)$ and $C(4)$ chains propagating along [100] and [010], respectively, which together generate (001) sheets. In the crystal of NOVGAI, inversion dimers linked by pairs of $\text{C}-\text{H}\cdots\text{O}$ hydrogen bonds generate $R_2^2(8)$ loops. In the crystal of WUFBEG, inversion dimers linked by pairs of $\text{C}-\text{H}\cdots\text{O}$ hydrogen bonds generate $R_2^2(10)$ loops. Additional intermolecular $\text{C}-\text{H}\cdots\text{O}$ hydrogen bonds generate $C(7)$ chains along [100]. In the crystal of EZOMIR, inversion dimers linked by pairs of $\text{N}-\text{H}\cdots\text{N}$ hydrogen bonds generate $R_2^2(12)$ loops.

5. Synthesis and crystallization

N-[*(E*)-(4-Fluorophenyl)methylidene]-4-bromaniline: Anhydrous MgSO_4 (3.61 g, 0.030 mol) and 4-fluorobenzaldehyde (1.86 g, 0.015 mol) were successively added to a solution of 4-bromaniline (2.60 g, 0.015 mol) in CH_2Cl_2 (35 mL). After 24 h at room temperature, the reaction mixture was filtered through a silica gel layer (2 × 3 cm), eluent – CH_2Cl_2 (2 × 25 mL). The solvent was evaporated under reduced pressure and the residue was recrystallized from hexane/EtOAc. Azomethine was obtained as a light-yellow powder in a yield of 92% (3.88 g).

1-[6-Bromo-2-(4-fluorophenyl)-1,2,3,4-tetrahydroquinolin-4-yl]pyrrolidin-2-one (1): Boron trifluoride ether (0.33 mL, 0.0026 mol) and *N*-vinylpyrrolidone (1.50 mL, 0.014 mol) were added to a cooled solution (275–277 K) of the previously obtained azomethine (3.50 g, 0.013 mol) in freshly distilled CH_2Cl_2 (30 mL). After that, the suspension was mixed at room temperature for 24 h and treated with a small amount of water (0.2–0.3 mL) to decompose the catalyst. The reaction mixture was filtered through a layer of silica gel (2 × 3 cm), washed with CH_2Cl_2 (2 × 6 mL) and the solvent was

**Figure 10**

The two-dimensional fingerprint plots for the title compound showing (a) all interactions, and delineated into (b) $\text{H}\cdots\text{H}$, (c) $\text{C}\cdots\text{H}/\text{H}\cdots\text{C}$, (d) $\text{Br}\cdots\text{H}/\text{H}\cdots\text{Br}$ and (e) $\text{F}\cdots\text{H}/\text{H}\cdots\text{F}$ interactions. The d_i and d_e values are the closest internal and external distances (in Å) from given points on the Hirshfeld surface.

evaporated under reduced pressure. The obtained product was recrystallized from a mixture of hexane/EtOAc. A white microcrystalline precipitate of the title compound was isolated in a yield of 43% (2.17 g), m.p. 460.3–462.3 K. IR (KBr), ν (cm⁻¹): 3344 (NH), 2956 (Ph), 2897 (Ph), 1666 (N—C=O). ¹H NMR (700 MHz, CDCl₃, 298 K) (*J*, Hz): δ 2.00–2.10 (*m*, 4H, H-3 + H-4-pyrrole), 2.43–2.47 (*m*, 1H, H-3-pyrrole-A), 2.52–2.57 (*m*, 1H, H-3-pyrrole-B), 3.19–3.26 (*m*, 2H, H-5-pyrrole), 4.56 (*dd*, *J* = 9.5, *J* = 5.0, 1H, H-2), 5.65–5.68 (*m*, 1H, H-4), 6.48 (*d*, *J* = 8.3, 1H, H-8), 6.95 (*br.s*, 1H, H-5), 7.05–7.08 (*m*, 2H, H-2,6-C₆H₄-F), 7.14 (*dd*, *J* = 8.6, *J* = 2.4, 1H, H-7), 7.38–7.40 (*m*, 2H, H-3,5-C₆H₄-F) ppm. ¹³C NMR{¹H} (176 MHz, CDCl₃, 298 K) (*J*, Hz): δ 18.18, 31.19, 34.82, 42.21, 48.07, 55.68, 110.10, 115.65 (*d*, 2C, ²J_{C,F} = 21.6), 116.67, 121.05, 128.06 (*d*, 2C, ³J_{C,F} = 8.1), 129.14, 131.10, 138.15 (*br.s*, 1C), 144.59, 162.38 (*d*, ¹J_{C,F} = 245.8), 175.84 ppm. ¹⁹F NMR{¹H} (659 MHz, CDCl₃, 298 K): δ –113.93 (*s*, 1F) ppm. Elemental analysis calculated (%) for C₁₉H₁₈BrFN₂O: C, 58.62; H, 4.66; N, 7.20; found: C, 58.73; H, 4.53; N, 7.15. Single crystals (colourless prisms) of the title compound were grown from a mixture of hexane and ethyl acetate (~3:1).

6. Refinement

Crystal data, data collection and structure refinement details are summarized in Table 2. The C-bound H atoms were placed in calculated positions (0.95–1.00 Å) and refined as riding with $U_{\text{iso}}(\text{H}) = 1.2U_{\text{eq}}(\text{C})$. The N-bound H atom was located in a difference map and freely refined.

Acknowledgements

This work was supported by the Western Caspian University (Azerbaijan), Azerbaijan Medical University and Baku State University. This publication was supported by the RUDN University Scientific Projects Grant System, project No. 021408-2-000. EDY and ERS thank the Common Use Center "Physical and Chemical Research of New Materials, Substances and Catalytic Systems". The authors' contributions are as follows. Conceptualization, MA and AB; synthesis, AAP and AGP; X-ray analysis, MSG, KIH and NDS; writing (review and editing of the manuscript) AAP, NDS, KIH and AGP; funding acquisition, AB and MA; supervision, MA and MSG.

References

- Abdelhamid, A. A., Mohamed, S. K., Khalilov, A. N., Gurbanov, A. V. & Ng, S. W. (2011). *Acta Cryst.* **E67**, o744.
 Akbari Afkhami, F., Mahmoudi, G., Gurbanov, A. V., Zubkov, F. I., Qu, F., Gupta, A. & Safin, D. A. (2017). *Dalton Trans.* **46**, 14888–14896.
 Astudillo, L., S., Gutiérrez Cabrera, M. I., Gaete, H., Kouznetsov, V. V., Meléndez, C. M., Palenzuela, J. A. & Vallejos, G. (2009). *Lett. Org. Chem.* **6**, 208–212.
 Bruker (2018). *APEX3* and *SAINT*. Bruker AXS Inc., Madison, Wisconsin, USA.
- Çelik, İ., Akkurt, M., Çakmak, O., Ökten, S. & García-Granda, S. (2010b). *Acta Cryst.* **E66**, o2997–o2998.
 Çelik, İ., Akkurt, M., Ökten, S., Çakmak, O. & García-Granda, S. (2010a). *Acta Cryst.* **E66**, o3133.
 Çelik, I., Ökten, S., Ersanlı, C. C., Akkurt, M. & Çakmak, O. (2016). *IUCrData*, **1**, x161854.
 Cremer, D. & Pople, J. A. (1975). *J. Am. Chem. Soc.* **97**, 1354–1358.
 Farrugia, L. J. (2012). *J. Appl. Cryst.* **45**, 849–854.
 Ghashghaei, O., Masdeu, C., Alonso, C., Palacios, F. & Lavilla, R. (2018). *Drug. Discov. Today: Technol.* **29**, 71–79.
 Groom, C. R., Bruno, I. J., Lightfoot, M. P. & Ward, S. C. (2016). *Acta Cryst.* **B72**, 171–179.
 Gurbanov, A. V., Kuznetsov, M. L., Karmakar, A., Aliyeva, V. A., Mahmudov, K. T. & Pombeiro, A. J. L. (2022a). *Dalton Trans.* **51**, 1019–1031.
 Gurbanov, A. V., Kuznetsov, M. L., Mahmudov, K. T., Pombeiro, A. J. L. & Resnati, G. (2020). *Chem. Eur. J.* **26**, 14833–14837.
 Gurbanov, A. V., Kuznetsov, M. L., Resnati, G., Mahmudov, K. T. & Pombeiro, A. J. L. (2022b). *Cryst. Growth Des.* **22**, 3932–3940.
 Jeyaseelan, S., Nagendra Babu, S. L., Venkateshappa, G., Raghavendra Kumar, P. & Palakshamurthy, B. S. (2015a). *Acta Cryst.* **E71**, o20.
 Jeyaseelan, S., Rajegowda, H. R., Britto Dominic Rayan, R., Raghavendra Kumar, P. & Palakshamurthy, B. S. (2015b). *Acta Cryst.* **E71**, 660–662.
 Jeyaseelan, S., Sowmya, B. R., Venkateshappa, G., Raghavendra Kumar, P. & Palakshamurthy, B. S. (2015c). *Acta Cryst.* **E71**, o249–o250.
 Khalilov, A. N., Tüzün, B., Taslimi, P., Tas, A., Tunçbilek, Z. & Çakmak, N. K. (2021). *J. Mol. Liq.* **344**, 117761.

- Kopylovich, M. N., Karabach, Y. Y., Mahmudov, K. T., Haukka, M., Kirillov, A. M., Figiel, P. J. & Pombeiro, A. J. L. (2011a). *Cryst. Growth Des.* **11**, 4247–4252.
- Kopylovich, M. N., Mahmudov, K. T., Haukka, M., Luzyanin, K. V. & Pombeiro, A. J. L. (2011b). *Inorg. Chim. Acta*, **374**, 175–180.
- Kouznetsov, V. V., Cruz, U. M., Zubkov, F. I. & Nikitina, E. V. (2007). *Synthesis*, **2007**, 375–384.
- Kouznetsov, V. V., Zubkov, F. I., Cruz, U. M., Voskressensky, L. G., Mendez, L. Y. V., Astudillo, L. & Stashenko, E. E. (2004). *Lett. Org. Chem.* **1**, 37–39.
- Krause, L., Herbst-Irmer, R., Sheldrick, G. M. & Stalke, D. (2015). *J. Appl. Cryst.* **48**, 3–10.
- Mahmoudi, G., Dey, L., Chowdhury, H., Bauzá, A., Ghosh, B. K., Kirillov, A. M., Seth, S. K., Gurbanov, A. V. & Frontera, A. (2017a). *Inorg. Chim. Acta*, **461**, 192–205.
- Mahmoudi, G., Zaręba, J. K., Gurbanov, A. V., Bauzá, A., Zubkov, F. I., Kubicki, M., Stilinović, V., Kinzhylbalo, V. & Frontera, A. (2017b). *Eur. J. Inorg. Chem.* pp. 4763–4772.
- Palacios, F., Alonso, C., Arrieta, A., Cossío, F. P., Ezpeleta, J. M., Fuertes, M. & Rubiales, G. (2010). *Eur. J. Org. Chem.* pp. 2091–2099.
- Safavora, A. S., Brito, I., Cisterna, J., Cárdenas, A., Huseynov, E. Z., Khalilov, A. N., Naghiyev, F. N., Askerov, R. K. & Maharramov, A. M. (2019). *Z. Kristallogr. New Cryst. Struct.* **234**, 1183–1185.
- Sheldrick, G. M. (2015a). *Acta Cryst. A* **71**, 3–8.
- Sheldrick, G. M. (2015b). *Acta Cryst. C* **71**, 3–8.
- Spackman, P. R., Turner, M. J., McKinnon, J. J., Wolff, S. K., Grimwood, D. J., Jayatilaka, D. & Spackman, M. A. (2021). *J. Appl. Cryst.* **54**, 1006–1011.
- Spek, A. L. (2020). *Acta Cryst. E* **76**, 1–11.
- Sridharan, V., Suryavanshi, P. A. & Menéndez, J. C. (2011). *Chem. Rev.* **111**, 7157–7259.
- Zaitsev, V. P., Mikhailova, N. M., Orlova, D. N., Nikitina, E. V., Boltukhina, E. V. & Zubkov, F. I. (2009). *Chem. Heterocycl. Compd.* **45**, 308–316.
- Zubkov, F. I., Zaitsev, V. P., Piskareva, A. M., Eliseeva, M. N., Nikitina, E. V., Mikhailova, N. M. & Varlamov, A. V. (2010). *Russ. J. Org. Chem.* **46**, 1192–1206.

supporting information

Acta Cryst. (2024). E80, 777-782 [https://doi.org/10.1107/S2056989024005826]

Crystal structure and Hirshfeld surface analysis of 1-[6-bromo-2-(4-fluorophenyl)-1,2,3,4-tetrahydroquinolin-4-yl]pyrrolidin-2-one

Anastasia A. Pronina, Alexandra G. Podrezova, Mikhail S. Grigoriev, Khudayar I. Hasanov, Nurlana D. Sadikhova, Mehmet Akkurt and Ajaya Bhattacharai

Computing details

1-[6-Bromo-2-(4-fluorophenyl)-1,2,3,4-tetrahydroquinolin-4-yl]pyrrolidin-2-one

Crystal data

$C_{19}H_{18}BrFN_2O$
 $M_r = 389.26$
Monoclinic, $P2_1/n$
 $a = 9.2092$ (6) Å
 $b = 9.0576$ (6) Å
 $c = 20.4085$ (13) Å
 $\beta = 101.518$ (2)°
 $V = 1668.06$ (19) Å³
 $Z = 4$

$F(000) = 792$
 $D_x = 1.550$ Mg m⁻³
Mo $K\alpha$ radiation, $\lambda = 0.71073$ Å
Cell parameters from 5298 reflections
 $\theta = 3.0\text{--}27.1^\circ$
 $\mu = 2.48$ mm⁻¹
 $T = 100$ K
Bulk, colourless
0.40 × 0.36 × 0.34 mm

Data collection

Bruker Kappa APEXII area-detector
diffractometer
 φ and ω scans
Absorption correction: multi-scan
(SADABS; Krause *et al.*, 2015)
 $T_{\min} = 0.752$, $T_{\max} = 1.000$
28015 measured reflections

4882 independent reflections
3713 reflections with $I > 2\sigma(I)$
 $R_{\text{int}} = 0.057$
 $\theta_{\max} = 30.1^\circ$, $\theta_{\min} = 3.8^\circ$
 $h = -12 \rightarrow 12$
 $k = -12 \rightarrow 12$
 $l = -28 \rightarrow 28$

Refinement

Refinement on F^2
Least-squares matrix: full
 $R[F^2 > 2\sigma(F^2)] = 0.035$
 $wR(F^2) = 0.072$
 $S = 1.02$
4882 reflections
221 parameters
0 restraints

Primary atom site location: structure-invariant
direct methods
Hydrogen site location: mixed
H atoms treated by a mixture of independent
and constrained refinement
 $w = 1/[\sigma^2(F_o^2) + (0.0267P)^2 + 0.8068P]$
where $P = (F_o^2 + 2F_c^2)/3$
 $(\Delta/\sigma)_{\max} = 0.001$
 $\Delta\rho_{\max} = 0.45$ e Å⁻³
 $\Delta\rho_{\min} = -0.40$ e Å⁻³

Special details

Geometry. All esds (except the esd in the dihedral angle between two l.s. planes) are estimated using the full covariance matrix. The cell esds are taken into account individually in the estimation of esds in distances, angles and torsion angles; correlations between esds in cell parameters are only used when they are defined by crystal symmetry. An approximate (isotropic) treatment of cell esds is used for estimating esds involving l.s. planes.

Fractional atomic coordinates and isotropic or equivalent isotropic displacement parameters (\AA^2)

	<i>x</i>	<i>y</i>	<i>z</i>	$U_{\text{iso}}^*/U_{\text{eq}}$
C2	0.64897 (19)	0.1250 (2)	0.42863 (9)	0.0113 (3)
H2A	0.664204	0.021487	0.445624	0.014*
C3	0.7094 (2)	0.2311 (2)	0.48563 (9)	0.0114 (4)
H3A	0.695266	0.334338	0.469667	0.014*
H3B	0.816813	0.213924	0.501577	0.014*
C4	0.62722 (19)	0.2058 (2)	0.54273 (9)	0.0098 (3)
H4A	0.639259	0.099050	0.555148	0.012*
C4A	0.46344 (19)	0.23196 (19)	0.51703 (9)	0.0097 (3)
C5	0.3722 (2)	0.2855 (2)	0.55836 (9)	0.0125 (4)
H5A	0.413562	0.314242	0.602937	0.015*
C6	0.2210 (2)	0.2968 (2)	0.53445 (10)	0.0132 (4)
C7	0.1569 (2)	0.2503 (2)	0.47072 (10)	0.0144 (4)
H7A	0.052477	0.253929	0.455694	0.017*
C8	0.2472 (2)	0.1984 (2)	0.42916 (10)	0.0127 (4)
H8A	0.204136	0.166365	0.385250	0.015*
C8A	0.4015 (2)	0.19234 (19)	0.45099 (9)	0.0110 (4)
C12	0.74202 (19)	0.2236 (2)	0.66142 (9)	0.0117 (4)
C13	0.8116 (2)	0.3412 (2)	0.70995 (10)	0.0170 (4)
H13A	0.921011	0.333787	0.718707	0.020*
H13B	0.777820	0.331985	0.752877	0.020*
C14	0.7601 (3)	0.4872 (2)	0.67578 (10)	0.0247 (5)
H14A	0.677041	0.529078	0.693974	0.030*
H14B	0.842211	0.559631	0.682281	0.030*
C15	0.7101 (2)	0.4493 (2)	0.60191 (10)	0.0146 (4)
H15A	0.617049	0.501351	0.582257	0.018*
H15B	0.787199	0.475484	0.576387	0.018*
C21	0.7300 (2)	0.1449 (2)	0.37154 (9)	0.0113 (4)
C22	0.8453 (2)	0.0493 (2)	0.36616 (10)	0.0144 (4)
H22A	0.866503	-0.031520	0.396188	0.017*
C23	0.9300 (2)	0.0700 (2)	0.31764 (10)	0.0169 (4)
H23A	1.008962	0.004965	0.314036	0.020*
C24	0.8955 (2)	0.1873 (3)	0.27535 (10)	0.0195 (4)
C25	0.7829 (2)	0.2849 (3)	0.27849 (11)	0.0251 (5)
H25A	0.762472	0.365242	0.248101	0.030*
C26	0.6999 (2)	0.2627 (2)	0.32732 (10)	0.0184 (4)
H26A	0.621590	0.328838	0.330588	0.022*
Br1	0.10063 (2)	0.37706 (2)	0.59152 (2)	0.02069 (7)
F1	0.97779 (13)	0.20988 (16)	0.22741 (6)	0.0311 (3)
N1	0.48956 (17)	0.15098 (18)	0.40598 (8)	0.0127 (3)

N11	0.68720 (16)	0.28987 (17)	0.60227 (7)	0.0101 (3)
O1	0.73676 (15)	0.09059 (14)	0.67215 (7)	0.0159 (3)
H1	0.446 (3)	0.094 (3)	0.3753 (12)	0.022 (6)*

Atomic displacement parameters (\AA^2)

	U^{11}	U^{22}	U^{33}	U^{12}	U^{13}	U^{23}
C2	0.0122 (8)	0.0126 (9)	0.0094 (9)	-0.0001 (7)	0.0027 (7)	0.0007 (7)
C3	0.0121 (8)	0.0117 (9)	0.0106 (9)	-0.0017 (7)	0.0029 (7)	-0.0004 (7)
C4	0.0124 (8)	0.0090 (9)	0.0084 (9)	-0.0013 (7)	0.0027 (7)	-0.0007 (7)
C4A	0.0128 (8)	0.0071 (8)	0.0094 (9)	-0.0022 (7)	0.0029 (7)	0.0016 (7)
C5	0.0159 (9)	0.0114 (9)	0.0106 (9)	-0.0022 (7)	0.0037 (7)	-0.0005 (7)
C6	0.0132 (9)	0.0111 (9)	0.0171 (10)	0.0006 (7)	0.0072 (8)	-0.0006 (7)
C7	0.0104 (8)	0.0125 (9)	0.0203 (10)	-0.0008 (7)	0.0030 (8)	0.0011 (8)
C8	0.0137 (9)	0.0105 (9)	0.0131 (9)	-0.0029 (7)	0.0007 (7)	-0.0011 (7)
C8A	0.0136 (9)	0.0069 (9)	0.0129 (9)	-0.0016 (7)	0.0039 (7)	0.0011 (7)
C12	0.0094 (8)	0.0164 (10)	0.0102 (9)	0.0024 (7)	0.0038 (7)	0.0011 (7)
C13	0.0177 (10)	0.0207 (11)	0.0113 (10)	-0.0011 (8)	-0.0001 (8)	-0.0019 (8)
C14	0.0411 (13)	0.0161 (11)	0.0148 (11)	-0.0047 (9)	0.0005 (10)	-0.0031 (8)
C15	0.0183 (9)	0.0106 (9)	0.0147 (10)	-0.0024 (7)	0.0027 (8)	-0.0012 (7)
C21	0.0126 (8)	0.0136 (10)	0.0071 (8)	-0.0010 (7)	0.0008 (7)	-0.0021 (7)
C22	0.0153 (9)	0.0138 (10)	0.0140 (10)	0.0004 (7)	0.0025 (8)	-0.0012 (8)
C23	0.0116 (9)	0.0220 (11)	0.0167 (10)	-0.0004 (8)	0.0016 (8)	-0.0069 (8)
C24	0.0140 (9)	0.0356 (12)	0.0103 (10)	-0.0018 (9)	0.0053 (8)	-0.0017 (9)
C25	0.0218 (11)	0.0363 (13)	0.0188 (11)	0.0066 (9)	0.0080 (9)	0.0138 (10)
C26	0.0162 (9)	0.0233 (11)	0.0171 (10)	0.0070 (8)	0.0064 (8)	0.0074 (8)
Br1	0.01630 (10)	0.02401 (11)	0.02408 (12)	0.00192 (9)	0.00963 (8)	-0.00610 (10)
F1	0.0234 (7)	0.0555 (9)	0.0186 (7)	0.0011 (6)	0.0141 (5)	0.0060 (6)
N1	0.0116 (7)	0.0173 (9)	0.0096 (8)	-0.0032 (6)	0.0026 (6)	-0.0037 (6)
N11	0.0137 (7)	0.0084 (7)	0.0079 (7)	-0.0002 (6)	0.0013 (6)	-0.0002 (6)
O1	0.0228 (7)	0.0126 (7)	0.0118 (7)	0.0042 (5)	0.0025 (6)	0.0031 (5)

Geometric parameters (\AA , °)

C2—N1	1.467 (2)	C12—C13	1.508 (3)
C2—C21	1.514 (2)	C13—C14	1.525 (3)
C2—C3	1.526 (2)	C13—H13A	0.9900
C2—H2A	1.0000	C13—H13B	0.9900
C3—C4	1.528 (2)	C14—C15	1.525 (3)
C3—H3A	0.9900	C14—H14A	0.9900
C3—H3B	0.9900	C14—H14B	0.9900
C4—N11	1.447 (2)	C15—N11	1.459 (2)
C4—C4A	1.513 (2)	C15—H15A	0.9900
C4—H4A	1.0000	C15—H15B	0.9900
C4A—C5	1.391 (2)	C21—C26	1.389 (3)
C4A—C8A	1.401 (3)	C21—C22	1.391 (3)
C5—C6	1.384 (3)	C22—C23	1.390 (3)
C5—H5A	0.9500	C22—H22A	0.9500

C6—C7	1.382 (3)	C23—C24	1.365 (3)
C6—Br1	1.9053 (18)	C23—H23A	0.9500
C7—C8	1.383 (3)	C24—F1	1.367 (2)
C7—H7A	0.9500	C24—C25	1.374 (3)
C8—C8A	1.403 (3)	C25—C26	1.386 (3)
C8—H8A	0.9500	C25—H25A	0.9500
C8A—N1	1.393 (2)	C26—H26A	0.9500
C12—O1	1.227 (2)	N1—H1	0.85 (2)
C12—N11	1.352 (2)		
N1—C2—C21	110.74 (14)	C14—C13—H13A	110.7
N1—C2—C3	109.20 (15)	C12—C13—H13B	110.7
C21—C2—C3	110.55 (14)	C14—C13—H13B	110.7
N1—C2—H2A	108.8	H13A—C13—H13B	108.8
C21—C2—H2A	108.8	C15—C14—C13	105.17 (17)
C3—C2—H2A	108.8	C15—C14—H14A	110.7
C2—C3—C4	109.03 (14)	C13—C14—H14A	110.7
C2—C3—H3A	109.9	C15—C14—H14B	110.7
C4—C3—H3A	109.9	C13—C14—H14B	110.7
C2—C3—H3B	109.9	H14A—C14—H14B	108.8
C4—C3—H3B	109.9	N11—C15—C14	103.49 (16)
H3A—C3—H3B	108.3	N11—C15—H15A	111.1
N11—C4—C4A	113.30 (14)	C14—C15—H15A	111.1
N11—C4—C3	113.41 (14)	N11—C15—H15B	111.1
C4A—C4—C3	108.86 (15)	C14—C15—H15B	111.1
N11—C4—H4A	107.0	H15A—C15—H15B	109.0
C4A—C4—H4A	107.0	C26—C21—C22	118.86 (17)
C3—C4—H4A	107.0	C26—C21—C2	121.75 (16)
C5—C4A—C8A	119.53 (17)	C22—C21—C2	119.20 (16)
C5—C4A—C4	121.70 (16)	C23—C22—C21	121.23 (18)
C8A—C4A—C4	118.66 (15)	C23—C22—H22A	119.4
C6—C5—C4A	119.94 (18)	C21—C22—H22A	119.4
C6—C5—H5A	120.0	C24—C23—C22	117.51 (18)
C4A—C5—H5A	120.0	C24—C23—H23A	121.2
C7—C6—C5	121.30 (17)	C22—C23—H23A	121.2
C7—C6—Br1	120.02 (14)	C23—C24—F1	118.44 (18)
C5—C6—Br1	118.67 (14)	C23—C24—C25	123.63 (18)
C6—C7—C8	118.99 (17)	F1—C24—C25	117.93 (19)
C6—C7—H7A	120.5	C24—C25—C26	118.0 (2)
C8—C7—H7A	120.5	C24—C25—H25A	121.0
C7—C8—C8A	120.88 (18)	C26—C25—H25A	121.0
C7—C8—H8A	119.6	C25—C26—C21	120.77 (18)
C8A—C8—H8A	119.6	C25—C26—H26A	119.6
N1—C8A—C4A	121.61 (16)	C21—C26—H26A	119.6
N1—C8A—C8	119.18 (17)	C8A—N1—C2	120.88 (16)
C4A—C8A—C8	119.19 (16)	C8A—N1—H1	113.3 (15)
O1—C12—N11	125.02 (18)	C2—N1—H1	115.7 (15)
O1—C12—C13	127.12 (17)	C12—N11—C4	121.86 (16)

N11—C12—C13	107.85 (16)	C12—N11—C15	114.52 (16)
C12—C13—C14	105.05 (16)	C4—N11—C15	123.22 (15)
C12—C13—H13A	110.7		
N1—C2—C3—C4	59.01 (19)	N1—C2—C21—C22	-140.90 (18)
C21—C2—C3—C4	-178.91 (15)	C3—C2—C21—C22	97.9 (2)
C2—C3—C4—N11	173.65 (15)	C26—C21—C22—C23	0.0 (3)
C2—C3—C4—C4A	-59.24 (19)	C2—C21—C22—C23	-175.11 (17)
N11—C4—C4A—C5	-22.0 (2)	C21—C22—C23—C24	-0.2 (3)
C3—C4—C4A—C5	-149.14 (17)	C22—C23—C24—F1	179.79 (18)
N11—C4—C4A—C8A	162.03 (16)	C22—C23—C24—C25	0.2 (3)
C3—C4—C4A—C8A	34.9 (2)	C23—C24—C25—C26	0.0 (3)
C8A—C4A—C5—C6	1.1 (3)	F1—C24—C25—C26	-179.62 (19)
C4—C4A—C5—C6	-174.83 (17)	C24—C25—C26—C21	-0.2 (3)
C4A—C5—C6—C7	2.6 (3)	C22—C21—C26—C25	0.2 (3)
C4A—C5—C6—Br1	-177.82 (14)	C2—C21—C26—C25	175.16 (19)
C5—C6—C7—C8	-3.2 (3)	C4A—C8A—N1—C2	9.6 (3)
Br1—C6—C7—C8	177.20 (14)	C8—C8A—N1—C2	-172.17 (17)
C6—C7—C8—C8A	0.1 (3)	C21—C2—N1—C8A	-156.30 (16)
C5—C4A—C8A—N1	174.11 (16)	C3—C2—N1—C8A	-34.3 (2)
C4—C4A—C8A—N1	-9.8 (3)	O1—C12—N11—C4	-5.8 (3)
C5—C4A—C8A—C8	-4.1 (3)	C13—C12—N11—C4	173.15 (15)
C4—C4A—C8A—C8	171.96 (16)	O1—C12—N11—C15	-178.77 (17)
C7—C8—C8A—N1	-174.75 (17)	C13—C12—N11—C15	0.2 (2)
C7—C8—C8A—C4A	3.5 (3)	C4A—C4—N11—C12	115.73 (18)
O1—C12—C13—C14	-169.00 (18)	C3—C4—N11—C12	-119.53 (17)
N11—C12—C13—C14	12.1 (2)	C4A—C4—N11—C15	-71.9 (2)
C12—C13—C14—C15	-19.0 (2)	C3—C4—N11—C15	52.8 (2)
C13—C14—C15—N11	18.7 (2)	C14—C15—N11—C12	-12.3 (2)
N1—C2—C21—C26	44.1 (2)	C14—C15—N11—C4	174.87 (16)
C3—C2—C21—C26	-77.1 (2)		

Hydrogen-bond geometry (Å, °)

Cg3 is the centroid of the C4A/C5—C8/C8A ring.

D—H···A	D—H	H···A	D···A	D—H···A
N1—H1···O1 ⁱ	0.85 (2)	2.43 (2)	3.217 (2)	154 (2)
C5—H5A···F1 ⁱⁱ	0.95	2.50	3.393 (2)	157
C23—H23A···O1 ⁱⁱⁱ	0.95	2.46	3.365 (2)	159
C15—H15B···Br1 ^{iv}	0.99	2.98	3.703 (2)	131
C2—H2A···Cg3 ⁱ	1.00	2.68	3.676 (2)	172
C15—H15A···Cg3 ^v	0.99	2.94	3.386 (2)	109
C15—H15B···Cg3 ^v	0.99	2.97	3.386 (2)	106

Symmetry codes: (i) $-x+1, -y, -z+1$; (ii) $x-1/2, -y+1/2, z+1/2$; (iii) $-x+2, -y, -z+1$; (iv) $x+1, y, z$; (v) $-x+1, -y+1, -z+1$.